Available online at www.sciencedirect.com
SCIENCE DIRECT
Thermochimica Acta 443 (2006) 189–196
thermochimica acta
www.elsevier.com/locate/tca

Thermodynamic properties of $BaCeO_3$ and $BaZrO_3$ at low temperatures

M. Ahrens *, J. Maier

Max-Planck-Institut für Festkörperforschung, Heisenbergstraße 1, D-70569 Stuttgart, Germany

Received 28 November 2005; received in revised form 18 January 2006; accepted 19 January 2006
Available online 28 February 2006

Abstract

Specific heat capacities (C_p) of polycrystalline samples of $BaCeO_3$ and $BaZrO_3$ have been measured from about 1.6 K up to room temperature by means of adiabatic calorimetry. We provide corrected experimental data for the heat capacity of $BaCeO_3$ in the range $T < 10$ K and, for the first time, contribute experimental data below 53 K for $BaZrO_3$. Applying Debye's T^3-law for $T \rightarrow 0$ K, thermodynamic functions as molar entropy and enthalpy are derived by integration. We obtain $C_p = 114.8$ (± 1.0) J mol^{-1} K^{-1}, $S^\circ = 145.8$ (± 0.7) J mol^{-1} K^{-1} for $BaCeO_3$ and $C_p = 107.0$ (± 1.0) J mol^{-1} K^{-1}, $S^\circ = 125.5$ (± 0.6) J mol^{-1} K^{-1} for $BaZrO_3$ at 298.15 K. These results are in overall agreement with previously reported studies but slightly deviating, in both cases. Evaluations of $C_p(T)$ yield Debye temperatures and identify deviations from the simple Debye-theory due to extra vibrational modes as well as anharmonicity. The anharmonicity turns out to be more pronounced at elevated temperatures for $BaCeO_3$. The characteristic Debye temperatures determined at $T = 0$ K are $\Theta_0 = 365$ (± 6) K for $BaCeO_3$ and $\Theta_0 = 402$ (± 9) K for $BaZrO_3$.

Keywords: Heat capacity; Thermal analysis; Adiabatic calorimetry; Perovskites

1. Introduction

The perovskite-type ternary oxides $BaCeO_3$ and $BaZrO_3$ are materials of relevance in various fields of technology. In nuclear safety studies they are of interest as they can be formed in the fuel of nuclear reactors at high temperatures [1,2]. The refractory properties of zirconates are of importance for high temperature applications, such as in the form of thermal barrier coatings [3]. Both, cerates and zirconates, when appropriately doped, have gained attention as potential high temperature proton conductors with applicabilities in fuel cells or hydrogen sensors [4,5]. Zirconates in particular are used as insulators in the electroceramic industry and are gaining importance for heterogeneous catalysis [6]. $BaZrO_3$ turned out to be an important crucible material for growing crystals of high T_C superconductors [7]. Thermodynamic properties are required to evaluate chemical stabilities of compounds in various environments. In this respect low temperature heat capacities, ranging from liquid helium temperatures up to ambient temperatures, are of importance, as they provide absolute entropy data also for the high temperature range (due to the third law of thermodynamics). To our present knowledge, for both $BaCeO_3$ and $BaZrO_3$ there is only a single report, each on specific heat capacities at low temperature. The study of Scholten and Schoonman on $BaCeO_3$ [8] covers a similar range of temperatures as the present work, while the study of King and Weller on $BaZrO_3$ [9,10] does not comprise temperatures below 53 K (a range where essential entropy contributions emerge from, about 10% of the value at room temperature). The purpose of this paper is to contribute new data sets of thermodynamical low temperature properties for both compounds, and to set out the differences to data already published.

2. Experimental

2.1. Materials

Polycrystalline $BaCeO_3$ was prepared by mixing stoichiometric amounts of CeO_2 and $BaCO_3$ powders (the former material was purchased from Alfa – purity 99.9%, the latter one from Merck – purity > 99%) and reacting them by annealing at 1100 °C for 1 h in air with subsequent milling, followed by further annealing at 1300 °C for 3 h in air. After anew milling the powder was sintered in an alumina-crucible at 1300 °C for 5 h in air. Phase analysis was achieved by XRD (Cu Kα) at room temperature. The X-ray diffraction pattern corresponded to the

* Corresponding author. Tel.: +49 711 689 1765; fax: +49 711 689 1722.
E-mail address: m.ahrens@fkf.mpg.de (M. Ahrens).

0040-6031/$ – see front matter © 2006 Elsevier B.V. All rights reserved.
doi:10.1016/j.tca.2006.01.020

orthorhombic cell of $BaCeO_3$ (ICSD code: 079628), no second phase was revealed within the limits of resolution. No impurities could be detected by EDX spectroscopy (detection limit ≈1%).

After grinding, the powder was uniaxially compacted into pellets, each weighing around 300 mg, under an applied pressure of about 500 MPa, and finally sintered at 1300 °C in air for 5 h. The final grain size, investigated by SEM, was in the range of 5–20 μm.

$BaZrO_3$ powder of 99.9% purity (grain size < 10 μm) was purchased from Aldrich Chemical Compounds. The powder was uniaxially pelletised and sintered in the same way as described above. The grain size was in the range of microns as well. A check by XRD revealed no impurity phases.

2.2. Low-temperature calorimetry

The specific heat capacities at constant pressure (C_p) were measured in custom-built low temperature vacuum calorimeters. These were immersed in a bath cryostat containing either liquid helium or liquid nitrogen, depending on the desired temperature range. The calorimeters were equipped with miniature sample holders. Each holder consisted of a copper frame and a platform made of a thin sapphire disc suspended by three cotton threads from the frame. The platform carried the sample on top and a thin film heater (evaporated stainless steel, resistance ca. 2 kΩ) on its lower side. In the calorimeter designed for temperatures ranging from about 1.5 K up to about 100 K, a calibrated Cernox resistive temperature sensor was placed on the lower side of the sapphire disc, in order to measure the sample temperature (CX-1050, Lake Shore). Temperatures below 4.2 K were achieved by pumping the liquid helium bath. For the temperature range from 77 K up to room temperature a sample holder equipped with a calibrated platinum miniature sensor (Pt-100, Rosemount) was used. Liquid nitrogen was the coolant in the latter case.

Each polycrystalline sample had the shape of a small thin disk of about 300 mg, with a diameter around 10 mm and thickness of about 1–2 mm. It was mounted on top of the sapphire platform using a minute amount of Apiezon N high vacuum grease (<10 mg) to provide good thermal contact. The addenda contributions of the empty sample holder ensemble and of the Apiezon N grease were determined in separate runs and subtracted from the raw data of each run with a sample. The peak-shaped anomaly of the grease at about 298 K was adequately taken into account [11].

For the measurements reported here the quasi-adiabatic (isoperibol) step-heating method (Nernst's method) was employed, using an isothermal shield control [12,13]. To obtain the heat capacity at a fixed temperature, the shield temperature was kept constant with residual drift rates of the base line being less than $\pm 10^{-5}$ K/s, first of all. Subsequently a known small heat quantity was applied to the sample while recording the resulting temperature rise. The predetermined temperature increment during each heat pulse increased gradually from about 10 mK at lowest temperatures to about 1.5 K at 300 K. In general, each heat pulse was accompanied by heat loss of the sample-addenda ensemble due to thermal conduction along the suspension of the sapphire plate and due to radiation. The latter becomes most prominent on approaching room temperature and can give rise to increased scattering of data. The effect of heat loss was taken into account by additionally recording the post-heating period (up to 120 s, depending on temperature) and applying a particular fitting procedure [13]. Thus a corrected temperature increment was obtained. The relaxation time constants for heat loss increased from about 10 s at 1.5 K to about 2000 s at 100 K, eventually dropping again to lower values when approaching room temperature (increased heat loss caused by radiation). Uncertainties for the heat capacities, due to fundamental instrumental inaccuracy, are estimated to lie in between 0.5 and 1%. Sample-to-sample reproducibility is about 0.5%.

3. Results and discussions

The experimental molar heat capacities curves $C_p(T)$ for polycrystalline $BaCeO_3$ and $BaZrO_3$ are displayed in Fig. 1 along with the literature data from Scholten and Schoonman [8] and King and Weller [9,10], respectively, which were up to now the only available low temperature data sets. The temperature dependence of C_p has been least squares fitted in the two temperature ranges, 1.6 K < T < 50 K and 50 K < T < 300 K using a sixth order polynomial of the form $C_p(T) = \sum_{n=0}^{6} A_n T^n$. The polynomial coefficients are given in Table 1. A careful check showed that the sixth order polynomial gives perfect fits only above 15 K, so that for lower temperatures the original experimental values ought to be addressed. The thermodynamical properties such as molar entropy and molar enthalpy were calculated by numerical integration of the original data to achieve highest accuracy. The temperature range, no more accessible (in our case T < 1.5 K), is usually completed by a T^3-extrapolation down to 0 K. We expanded this range from 0 K to about 4 K as the experimental data deviate from the simple Debye law below 4 K (see Section 3.2). The experimental values of the heat capac-

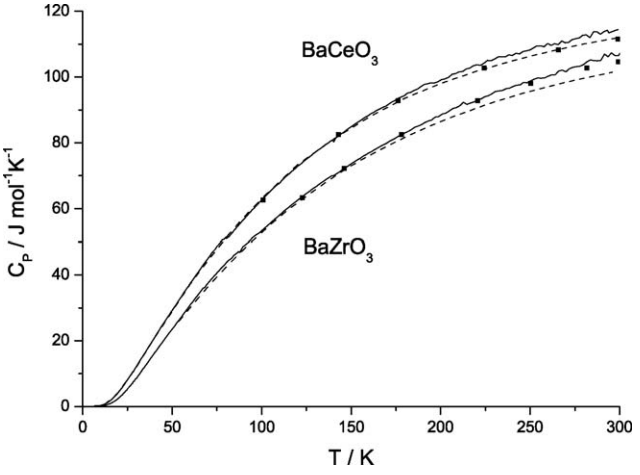

Fig. 1. The low temperature molar heat capacities of $BaCeO_3$ (m = 332.6 mg) and $BaZrO_3$ (m = 283.8 mg) as a function of temperature. Solid lines, present results; dashed lines, results according to Scholten and Schoonman ($BaCeO_3$) [8] and King and Weller ($BaZrO_3$) [9,10]; filled squares, calculated data (cf. Section 3.3).

Table 1
Polynomial coefficients for fitting the experimental heat capacities of $BaCeO_3$ and $BaZrO_3$ (see text)

Temperature range coefficients, A_i	1.6 K < T < 50 K	50 K < T < 300 K
$BaCeO_3$		
A_0	−0.3362	−37.01579
A_1	0.25729	2.00971
A_2	−0.06003	−0.0194
A_3	0.0056	1.42474×10^{-4}
A_4	-1.78046×10^{-4}	-6.27292×10^{-7}
A_5	2.56495×10^{-6}	1.42957×10^{-9}
A_6	-1.41793×10^{-8}	-1.29568×10^{-12}
$BaZrO_3$		
A_0	−0.23659	−33.28014
A_1	0.17299	1.61639
A_2	−0.03467	−0.01275
A_3	0.00263	7.36338×10^{-5}
A_4	-5.81273×10^{-5}	-2.49777×10^{-7}
A_5	4.74266×10^{-7}	4.24408×10^{-10}
A_6	-7.56029×10^{-10}	-2.64766×10^{-13}

ities are listed in Table 2 ($BaCeO_3$) and Table 3 ($BaZrO_3$). The absolute molar entropies $S^\circ(T)$ and the relative molar enthalpies $H^\circ(T) - H^\circ(298.15\,K)$, along with C_p, are listed at selected temperatures in Tables 4 and 5 by interpolating the data obtained from integration.

No phase transitions were detected within the investigated temperature range for both substances. This is in accordance with literature, reporting $BaCeO_3$ to maintain its low temperature orthorhombic structure up to 563 K [14,15] and $BaZrO_3$ to remain cubic down to lowest temperatures [16–18]. Note: the distinct kink in the $C_p(T)$ curve of $BaCeO_3$ around 79 K is an artefact, incidentally caused by the ceasing accuracy of the Cernox-resistor when approaching higher temperatures in combination with a change of calorimeters (changeover from liquid helium to liquid nitrogen). This deviation should not be taken too serious regarding the overall accuracy of the equipment.

3.1. Heat capacities and standard values at elevated temperatures

Compared to literature data, provided by Scholten and Schoonman and King and Weller, we find significantly higher heat capacity values above 200 K for both substances (beyond the limits of tolerance). In the case of $BaCeO_3$ our polynomial fit yields a smoothed value of 114.8 (±1.0) J mol^{-1} K^{-1} at 298.15 K, while Scholten and Schoonman [8] quote 111.9 (±0.2) J mol^{-1} K^{-1}. For $BaZrO_3$ we obtain 107.0 (±1.0) J mol^{-1} K^{-1} at 298.15 K, exceeding the value from King and Weller [9,10], 101.71 (±0.31) J mol^{-1} K^{-1}, by more than 5% (as their original data set only extends up to 296.08 K, the value at 298.15 K was obtained by slight extrapolation).

In the publication of King and Weller the heat capacity curve of $BaZrO_3$ is unexpectedly dropping below the one for $SrZrO_3$ above 240 K, instead of remaining on a higher level. This fact casts some doubt on the correctness of these data (the diagram referred to is also displayed in [19]). Comparing the standard molar entropy at room temperature, deviations are less significant: in the case of $BaCeO_3$ we find 145.8 (±0.7) J mol^{-1} K^{-1} at 298.15 K, while the studies of Scholten and Schoonman give 144.5 (±0.3) J mol^{-1} K^{-1}. For $BaZrO_3$ the measurement of King and Weller yields 124.7 (±1.3) J mol^{-1} K^{-1}, whereas we get 125.5 (±0.6) J mol^{-1} K^{-1}.

A compilation of data taken from literature for heat capacity and standard entropy at 298.15 K is presented in Table 6 along with our results. Concerning $BaCeO_3$ the data of Scholten and Schoonman [8] are, beside our study, the only ones gained by adiabatic calorimetry. The values of Saha et al. and Matsui [20,21] are merely estimates, obtained by adding the corresponding numbers of the constituent oxides according to the Neumann–Kopp rule. Krishnan et al. [22] applied high temperature DSC and determined the C_p value at room temperature by backward extrapolation. The molar standard entropy again was calculated by means of the Neumann–Kopp rule. Unsurprisingly, entropy values arrived at by this method exhibit severe deviations from the others.

In the case of $BaZrO_3$ the values quoted in Table 6, e.g. those taken from the data charts of Barin [23] and Knacke et al. [24], are mainly based on the original work of King and Weller, in which adiabatic calorimetry was applied. As their measurements did not extend below 53 K, the heat capacities in this range, finally contributing to the standard entropy at 298.15 K, were estimated by a particular fitting procedure. The value of Yamanaka et al. [25] was calculated from the extrapolated fit of a high temperature DSC measurement.

3.2. Heat capacities below 100 K

In the low temperature range our experimental results for $BaZrO_3$ match quite well with the data set of King and Weller (deviations are insignificant). Comparison below 53 K is not possible due to the aforementioned lack of data.

Regarding the results from Scholten and Schoonman for $BaCeO_3$, significant discrepancies are found below 20 K. Around 6.5 K we obtain $C_p = 0.064$ J mol^{-1} K^{-1} while Scholten and Schoonman report 0.20 J mol^{-1} K^{-1}. Similar to these authors we found excess specific heats at low temperatures, when initially investigating a powder sample of $BaCeO_3$, sealed in a glass ampoule along with helium for the purpose of good thermal coupling (see below). So far the origin of this excess heat could not be clarified (an adsorbed helium layer on the particle surfaces might be a cause).

A C_p/T^3 versus T plot, usually used to emphasise departures from Debye-like behaviour, is depicted in Fig. 2. The occurrence of a broad maximum, common to all samples, is in general related to the first maximum in the phonon density of states, giving rise to extra specific heat. The diagram reveals nice coincidence between our data and those by Scholten and Schoonman down to about 20 K. Additionally, a run with one of our powder samples is included, showing the aforementioned, distinct deviation from the pellet behaviour below 10 K in form of a second maximum. Finally the values are again joining those for the pellet at about 4 K. The values of Scholten and Schoonman show an even stronger increase, proceeding down to the

Table 2
Low temperature molar heat capacity of $BaCeO_3$

T	C_p	T	C_p	T	C_p	T	C_p	T	C_p	T	C_p
1.721	0.00113	7.04	0.0831	18.03	3.16	40.30	21.1	97.68	61.3	179.71	94.3
1.726	0.00106	7.13	0.0857	18.27	3.30	41.10	21.8	98.65	61.9	181.50	95.2
1.733	0.00113	7.24	0.0907	18.52	3.44	41.92	22.5	99.64	62.4	183.31	95.3
1.761	0.00102	7.34	0.0935	18.76	3.58	42.76	23.2	100.64	63.0	185.15	95.9
1.781	0.00108	7.45	0.0993	19.00	3.73	43.61	24.0	101.64	63.6	187.00	96.4
1.833	0.00116	7.55	0.103	19.23	3.89	44.48	24.7	102.66	64.1	188.86	97.1
1.870	0.00103	7.66	0.110	19.47	4.05	45.36	25.5	103.69	64.7	190.75	97.8
1.904	0.00103	7.76	0.115	19.73	4.19	46.27	26.2	104.72	65.2	192.65	98.0
1.995	0.00167	7.89	0.123	19.98	4.35	47.24	26.9	105.77	65.8	194.58	98.2
2.042	0.00152	8.00	0.129	20.20	4.52	48.19	27.7	106.83	66.4	196.52	98.2
2.096	0.00138	8.13	0.138	20.44	4.68	49.16	28.5	107.90	66.9	198.48	98.6
2.134	0.00153	8.25	0.145	20.69	4.84	50.15	29.4	108.97	67.4	200.46	99.2
2.178	0.00190	8.38	0.156	20.94	5.00	51.15	30.2	110.06	67.7	202.45	99.5
2.817	0.00505	8.50	0.164	21.17	5.20	52.16	31.0	111.16	68.5	204.43	100.0
2.844	0.00578	8.64	0.176	21.41	5.36	53.16	31.8	112.27	69.1	206.42	101.0
2.877	0.00560	8.77	0.185	21.66	5.54	54.16	32.6	113.40	69.7	208.40	101.1
3.154	0.00691	8.91	0.201	21.91	5.70	55.16	33.5	114.53	70.2	210.39	101.6
3.175	0.00697	9.04	0.209	22.16	5.88	56.16	34.3	115.68	70.8	212.37	101.7
3.250	0.00798	9.17	0.221	22.39	6.07	57.16	35.1	116.83	71.4	214.35	102.5
3.258	0.00871	9.32	0.241	22.63	6.26	58.15	35.9	118.00	71.9	216.33	102.8
3.318	0.00829	9.46	0.251	22.88	6.44	59.14	36.7	119.18	72.4	218.31	103.5
3.349	0.00913	9.59	0.266	23.14	6.62	60.13	37.4	120.37	73.0	220.30	103.8
3.382	0.00944	9.75	0.289	23.38	6.81	61.12	38.2	121.58	73.5	222.28	103.6
3.471	0.00930	9.92	0.309	23.62	7.00	62.11	39.0	122.79	74.0	224.26	104.2
3.570	0.0100	10.08	0.328	23.86	7.20	63.10	39.7	124.02	74.6	226.23	105.1
3.673	0.0107	10.23	0.348	24.10	7.39	64.09	40.5	125.26	75.1	228.22	105.0
3.834	0.0118	10.40	0.377	24.36	7.58	65.08	41.3	126.51	75.7	230.20	105.5
3.983	0.0132	10.58	0.400	24.61	7.76	66.07	42.0	127.77	76.2	232.17	106.2
4.140	0.0143	10.76	0.433	24.86	7.96	67.07	42.8	129.05	76.8	234.15	106.2
4.241	0.0157	10.94	0.461	25.10	8.19	68.06	43.6	130.34	77.3	236.14	106.1
4.384	0.0171	11.10	0.489	25.34	8.40	69.05	44.3	131.64	77.9	238.10	106.8
4.454	0.0187	11.30	0.534	25.60	8.57	70.05	45.0	132.96	78.4	240.08	106.6
4.608	0.0193	11.48	0.561	25.86	8.77	71.04	45.8	134.29	78.9	242.05	107.3
4.680	0.0211	11.68	0.610	26.10	8.98	72.03	46.6	135.63	79.4	244.02	107.1
4.756	0.0223	11.89	0.651	26.34	9.19	73.03	47.3	136.99	79.9	245.99	107.7
4.835	0.0232	12.09	0.700	26.57	9.41	74.02	47.8	138.36	80.4	249.95	108.3
4.911	0.0245	12.29	0.744	26.83	9.60	75.02	48.6	139.74	80.9	251.89	108.9
4.992	0.0260	12.50	0.806	27.09	9.80	76.02	49.2	141.54	81.6	253.89	109.5
5.071	0.0274	12.72	0.859	27.35	9.96	77.02	49.9	142.95	82.2	255.86	109.5
5.152	0.0284	12.93	0.919	27.60	10.2	78.02	50.6	144.38	82.8	257.84	109.2
5.227	0.0294	13.15	0.983	27.83	10.4	79.01	50.7	145.83	83.2	259.80	110.2
5.296	0.0316	13.37	1.05	28.07	10.7	80.01	51.5	147.28	83.8	261.77	109.7
5.375	0.0321	13.59	1.12	28.33	10.8	80.29	51.0	148.76	84.5	263.74	110.1
5.441	0.0353	13.82	1.20	28.59	10.7	81.69	51.5	150.25	85.0	267.67	111.0
5.536	0.0361	14.05	1.28	28.92	11.3	82.49	52.0	151.75	85.6	269.63	110.4
5.614	0.0388	14.28	1.36	29.29	11.6	83.31	52.5	153.27	86.1	271.61	110.6
5.697	0.0405	14.51	1.45	29.83	12.1	84.14	53.1	154.80	86.6	273.57	111.4
5.780	0.0425	14.74	1.54	30.39	12.6	84.98	53.7	156.34	87.3	275.53	111.7
5.861	0.0448	14.97	1.63	30.99	13.1	85.82	54.2	157.91	87.8	277.50	111.9
5.946	0.0466	15.21	1.73	31.60	13.6	86.68	54.7	159.49	88.2	279.46	112.8
6.034	0.0491	15.44	1.83	32.23	14.1	87.55	55.3	161.08	88.9	281.42	112.8
6.119	0.0516	15.68	1.93	32.89	14.7	88.43	55.8	162.69	89.3	283.39	112.0
6.209	0.0536	15.91	2.05	33.56	15.3	89.31	56.3	164.32	89.9	285.35	114.0
6.297	0.0571	16.15	2.16	34.26	15.9	90.21	56.9	165.96	90.3	287.30	114.2
6.366	0.0570	16.38	2.26	34.97	16.5	91.11	57.4	167.62	90.8	289.27	113.1
6.457	0.0616	16.60	2.38	35.70	17.1	92.02	58.0	169.30	91.2	291.22	113.8
6.548	0.0639	16.84	2.51	36.44	17.8	92.94	58.5	170.99	91.8	293.17	114.3
6.647	0.0675	17.09	2.62	37.19	18.4	93.87	59.1	172.70	92.4	294.05	113.5
6.739	0.0705	17.32	2.75	37.95	19.1	94.81	59.7	174.43	92.9	297.48	114.1
6.841	0.0743	17.55	2.89	38.72	19.8	95.75	60.2	176.17	93.5	299.16	114.5
6.930	0.0778	17.79	3.02	39.50	20.4	96.71	60.8	177.93	94.0		

T is in K; C_p is in $J\,mol^{-1}\,K^{-1}$.

Table 3
Low temperature molar heat capacity of $BaZrO_3$

T	C_p	T	C_p	T	C_p	T	C_p	T	C_p	T	C_p
1.659	0.00346	5.79	0.0301	13.93	0.599	28.32	7.57	82.18	44.7	185.48	84.7
1.662	0.00357	5.87	0.0306	14.13	0.628	28.59	7.63	83.18	45.1	187.34	85.1
1.664	0.00348	5.93	0.0325	14.34	0.692	28.82	7.79	84.17	45.7	189.21	85.5
1.666	0.00351	6.02	0.0336	14.54	0.702	29.03	8.03	85.17	46.3	191.10	86.2
1.671	0.00353	6.08	0.0338	14.75	0.772	29.26	8.25	86.17	46.7	193.00	86.7
1.675	0.00351	6.19	0.0357	14.97	0.803	30.34	8.73	87.17	47.2	194.93	87.0
1.677	0.00363	6.27	0.0366	15.18	0.858	30.07	8.73	87.74	46.8	196.88	87.9
1.683	0.00349	6.36	0.0388	15.39	0.892	30.45	8.93	89.50	48.5	198.84	88.0
1.689	0.00342	6.45	0.0407	15.59	0.951	31.03	9.36	91.29	49.3	200.83	88.7
1.699	0.00335	6.54	0.0424	15.81	1.02	31.64	9.80	93.12	50.1	202.81	89.0
1.722	0.00326	6.62	0.0440	16.03	1.06	32.28	10.4	94.99	51.3	204.80	89.7
1.735	0.00341	6.72	0.0458	16.24	1.13	32.94	10.9	96.90	52.1	206.78	90.5
1.744	0.00345	6.80	0.0494	16.46	1.20	33.63	11.4	98.84	52.7	208.76	90.8
1.763	0.00333	6.90	0.0501	16.68	1.25	34.33	11.9	100.82	53.7	210.75	91.3
2.098	0.00292	6.98	0.0511	16.90	1.32	35.05	12.4	102.81	54.6	212.73	92.4
2.107	0.00345	7.08	0.0539	17.12	1.40	35.78	13.0	104.80	55.6	214.71	91.7
2.124	0.00373	7.16	0.0547	17.34	1.46	36.53	13.5	106.79	56.6	216.70	92.1
2.150	0.0036	7.26	0.0547	17.56	1.54	37.28	14.1	108.78	57.5	218.69	92.5
2.163	0.00346	7.36	0.0593	17.79	1.63	38.03	14.7	110.77	58.4	220.66	93.0
2.173	0.00343	7.47	0.0629	18.03	1.72	38.80	15.3	112.76	59.4	222.65	93.4
2.185	0.00389	7.56	0.0638	18.26	1.77	39.58	15.9	114.75	60.3	224.62	94.0
2.198	0.00355	7.67	0.0662	18.47	1.87	40.37	16.4	116.74	61.2	226.60	94.3
2.209	0.00288	7.77	0.0700	18.69	1.97	41.18	17.1	118.72	62.0	228.58	94.9
2.216	0.00344	7.89	0.0767	18.92	2.07	42.00	17.7	120.69	62.8	230.56	95.7
2.228	0.00346	7.98	0.0760	19.15	2.15	42.84	18.3	122.66	63.7	232.54	95.8
2.261	0.00391	8.10	0.0841	19.38	2.27	43.69	19.0	124.65	64.5	234.52	95.9
2.281	0.0035	8.20	0.0830	19.62	2.37	44.56	19.6	126.64	65.3	236.49	96.5
2.325	0.00371	8.32	0.0910	19.86	2.44	45.45	20.2	128.63	66.1	238.47	96.6
2.372	0.0038	8.43	0.0913	20.07	2.59	46.36	21.0	130.62	66.8	240.44	97.1
2.389	0.00365	8.55	0.101	20.32	2.69	47.29	21.6	132.27	67.5	242.41	97.6
2.420	0.00384	8.67	0.102	20.56	2.75	48.24	22.3	133.60	68.0	244.39	97.6
2.515	0.00414	8.80	0.112	20.77	2.91	49.21	23.0	134.94	68.5	246.36	98.4
2.651	0.00484	8.91	0.111	21.00	3.03	50.25	23.7	136.28	69.0	248.33	98.2
2.824	0.00516	9.05	0.127	21.25	3.10	51.26	24.4	137.64	69.5	250.31	98.9
2.831	0.00564	9.12	0.121	21.47	3.28	52.27	25.2	139.02	70.0	252.27	99.4
2.919	0.00559	9.26	0.138	21.71	3.37	53.27	25.9	140.41	70.1	254.25	99.7
2.952	0.00633	9.33	0.130	21.95	3.48	54.27	26.6	141.81	70.6	256.22	99.7
3.106	0.00618	9.47	0.148	22.17	3.66	55.27	27.3	143.23	71.1	258.19	99.8
3.116	0.00718	9.60	0.144	22.41	3.78	56.27	28.1	144.66	71.7	260.16	100.3
3.242	0.00714	9.75	0.163	22.67	3.87	57.27	28.8	146.11	72.2	262.12	100.7
3.366	0.00794	9.88	0.159	22.90	3.98	58.26	29.5	147.57	72.7	264.08	100.7
3.538	0.00865	10.01	0.170	23.11	4.17	59.25	30.2	149.04	73.2	266.04	101.8
3.656	0.00903	10.18	0.188	23.34	4.32	60.25	31.0	150.53	73.9	268.01	102.2
3.873	0.00964	10.31	0.186	23.59	4.41	61.24	31.6	152.03	74.3	269.99	101.6
3.987	0.0104	10.47	0.208	23.83	4.56	62.30	32.5	153.55	74.9	271.94	102.6
4.096	0.0108	10.60	0.205	24.06	4.76	63.25	33.2	155.09	75.3	273.90	103.0
4.199	0.0112	10.76	0.228	24.31	4.87	64.23	33.8	156.64	75.9	275.86	103.2
4.473	0.0129	10.94	0.235	24.56	4.97	65.21	34.5	158.20	76.3	277.83	103.3
4.617	0.0156	11.09	0.245	24.78	5.12	66.20	35.2	159.79	76.9	279.79	103.8
4.702	0.0156	11.27	0.270	25.00	5.34	67.19	35.9	161.38	77.3	281.74	104.6
4.777	0.0158	11.45	0.278	25.24	5.49	68.19	36.2	163.00	77.9	283.71	105.2
4.851	0.0176	11.62	0.290	25.50	5.60	69.19	36.9	164.63	78.4	285.68	105.0
4.929	0.0183	11.80	0.317	25.74	5.74	71.18	38.3	166.26	78.9	287.63	105.0
5.008	0.0200	12.00	0.341	25.96	5.93	72.18	38.8	167.93	79.4	289.59	105.2
5.086	0.0190	12.15	0.340	26.19	6.12	73.19	39.5	169.61	79.9	291.54	107.0
5.165	0.0210	12.35	0.385	26.44	6.29	74.19	40.0	171.30	80.4	293.51	106.2
5.246	0.0226	12.54	0.383	26.70	6.36	75.18	40.7	173.01	81.0	295.49	107.4
5.329	0.0234	12.72	0.416	26.94	6.51	76.18	41.3	174.74	81.4	297.42	106.6
5.410	0.0243	12.92	0.449	27.15	6.76	77.18	42.0	176.49	82.0	299.39	106.6
5.489	0.0216	13.12	0.466	27.39	6.91	78.18	42.5	178.25	82.3	301.32	107.9
5.545	0.0289	13.32	0.500	27.72	7.04	79.18	43.1	180.03	83.0		
5.640	0.0269	13.53	0.540	27.68	6.91	80.18	43.6	181.83	83.5		
5.717	0.0288	13.73	0.561	28.07	7.40	81.18	44.3	183.65	84.1		

T is in K, C_p is in $J\,mol^{-1}\,K^{-1}$.

Table 4
Thermodynamic data of $BaCeO_3$ at selected temperatures

T	C_p	S^o	$H^\circ - H^\circ(298.15\,K)$
10	0.318	0.084	−21903
20	4.411	1.242	−21883
30	12.33	4.425	−21802
40	21.08	9.136	−21636
50	29.66	14.71	−21386
60	37.42	20.80	−21051
70	44.66	27.13	−20639
80	51.20	33.51	−20160
90	57.18	39.88	−19618
100	62.70	46.20	−19019
120	72.61	58.56	−17664
140	81.20	70.43	−16124
160	88.53	81.77	−14426
180	94.63	92.55	−12596
200	99.59	102.8	−10656
220	103.6	112.5	−8626
240	106.9	121.7	−6523
260	109.9	130.4	−4360
280	112.6	138.6	−2142
298.15	114.8	145.8	0.0
300	114.9	146.6	130.2

T is in K, C_p and S° are in J mol^{-1} K^{-1}, H° is in J mol^{-1}.

lowest accessible temperature. From the diagram we derive 2.0 (±0.1) × 10^{-4} J mol^{-1} K^{-4} for the prefactor of Debye's T^3-law, taking the limiting value of C_p/T^3 for $T \rightarrow 0$ K, whereas the increasing data points below 4 K are discarded. This increase may be due to grain boundary contributions, respectively disorder in general, or minute amounts of impurities (<1‰). These give rise to deviations from the simple Debye theory and become pronounced at low temperature [26–29]. The same value of the prefactor is obtained from the slope of a C_p/T versus T^2

Table 5
Thermodynamic data of $BaZrO_3$ at selected temperatures

T	C_p	S°	$H^\circ - H^\circ(298.15\,K)$
10	0.168	0.053	−19393
20	2.564	0.666	−19373
30	8.651	2.753	−19319
40	16.19	6.284	−19194
50	23.59	10.70	−18995
60	30.79	15.67	−18724
70	37.33	20.91	−18383
80	43.22	26.27	−17980
90	48.58	31.67	−17521
100	53.49	37.05	−17011
120	62.30	47.64	−15852
140	70.04	57.88	−14527
160	76.91	67.72	−13057
180	82.99	77.16	−11457
200	88.29	86.23	−9744
220	92.87	94.92	−7933
240	96.81	103.2	−6036
260	100.3	111.2	−4066
280	103.7	118.8	−2029
298.15	107.0	125.5	0.0
300	107.4	126.2	78.97

T is in K, C_p and S° are in J mol^{-1} K^{-1}, H° is in J mol^{-1}.

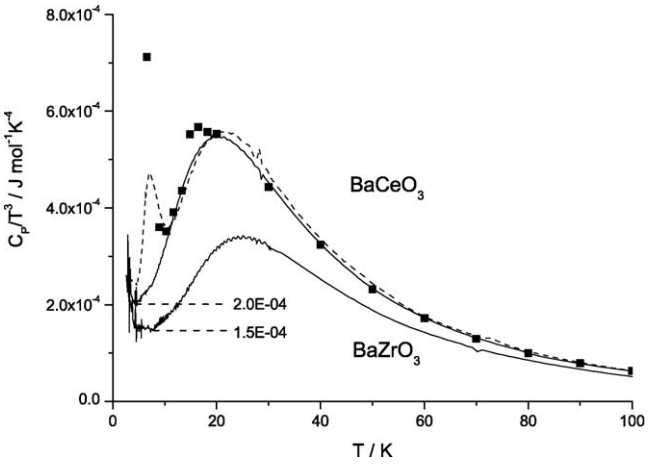

Fig. 2. Plots of C_p/T^3 vs. T for $BaCeO_3$ and $BaZrO_3$. Solid lines, present results; dashed line, result for a powder sample of $BaCeO_3$ (m = 295.2 mg); filled squares, data calculated from the results of Scholten and Schoonman [8].

plot below 25 K (not displayed), confirming this result. For the T^3-extrapolation below 10 K, Scholten and Schoonman used a Debye prefactor of 3.8 × 10^{-4} J mol^{-1} K^{-4}. Accordingly, the integration over this interval provides no proper entropy values for this range of temperatures (the effect on the standard value at 298.15 K is neglibible, of course). In their work they give 0.1256 J mol^{-1} K^{-1} for the molar entropy at 10 K, while we find 0.0844 J mol^{-1} K^{-1}.

In the case of $BaZrO_3$ the prefactor of Debye's T^3-law turns out to be 1.5 (±0.1) × 10^{-4} J mol^{-1} K^{-4}.

On interpreting the maximum of a C_p/T^3 curve in terms of an "Einstein-mode", the excess heat capacity (obtained after subtraction of the Debye contribution from the original experimental values) is usually fitted by the expression $\Delta C_p = 3Rm[\theta_E/2T\,\mathrm{csch}(\theta_E/2T)]^2$ [30,31]. Here R is the gas constant, θ_E the characteristic Einstein temperature and m is the weight factor, approximately representing the fraction of modes in the anomalous regime, which add to the simplified Debye spectrum (θ_E is related to the average frequency of the anomaly by $h\nu_E = k_B\theta_E$). For the fit we applied the approximation $\Delta C_p = 3Rm(\theta_E/2T)^2 \exp(-\theta_E/2T)$ valid for $T < \theta_E/4$, imposing 4 K as a lower limit (because of the aforementioned deviations below this temperature). We thus find θ_E = 101.8 (±0.2) K for $BaCeO_3$ and θ_E = 124.8 (±0.2) K for $BaZrO_3$. In theory the maximum of the C_p/T^3 versus T plot is approximately located at $T = \theta_E/5$, in accordance with our results. We want to mention the recent studies of Akbarzadeh et al. on $BaZrO_3$ presenting calculated phonon dispersion curves [18] (cf. Fig. 2 in this ref.). The estimated maximum of the phonon density-of-states satisfactorily agrees with the related Einstein temperature, derived above. The weight factor m is nearly the same for both compounds (0.7), indicating a typical property for perovskite-type oxides. It is interesting to note that θ_E, respectively ν_E, nearly scales with the inverse square root of the mass M of the transition metal atom: $(M_{Ce}/M_{Zr})^{-0.5} \cong \theta_E^{BaCeO_3}/\theta_E^{BaZrO_3} \cong 1.24$. An analogous relation between θ_E and M has already been observed for other transition metal compounds by Roedhammer et al. [31]. A fur-

Table 6
Thermodynamic properties of $BaCeO_3$ and $BaZrO_3$ at 298.15 K. Comparison of present results with data taken from literature

Compound	C_p (J mol^{-1} K^{-1})	S° (J mol^{-1} K^{-1})	Reference	Type of data
$BaCeO_3$ (325.46 g/mol)	114.8	145.8	This study	Adiabatic cal.
	111.9	144.50	[8]	Adiabatic cal.
	111.13	131.80	[20,21]	Neumann–Kopp
	109.2	134.37	[22]	DSC, Neumann–Kopp
$BaZrO_3$ (276.53 g/mol)	107.0	125.5	This study	Adiabatic cal.
	101.71	124.68	[9,10]	Adiabatic cal.
	100.71	124.683	[23]	Intern. consist. database
	105.39	124.683	[24]	Intern. consist. database
	107.71		[25]	DSC

ther discussion of the modes of lattice vibrations in perovskites would be beyond the scope of the paper.

3.3. Debye temperatures

Fig. 3 shows the temperature dependence of the Debye temperature θ_D, calculated from $C_p(T)$ by solving the equation $C_p(T) = 3RND[\theta_D(T)/T]$. Here D denotes the Debye function, e.g. tabulated in [30], while N is the number of atoms per formula unit (in the present case $N = 5$).

The displayed curves exhibit the typical shape [30]. The simple Debye phonon contribution is characterised by the limit of θ_D for $T \rightarrow 0$ K, termed θ_0. By extrapolating $\theta_D(T)$ towards $T = 0$ K we find $\theta_0 = 365$ (±6) K for $BaCeO_3$ and $\theta_0 = 402$ (±9) K for $BaZrO_3$. Usually the minimum of the C_p/T^3 versus T curve occurs around $\theta_0/20$, which is in agreement with our experiments. Sometimes, in literature, the conversion of specific heat data to Debye temperatures is accomplished by setting $N = 1$ in the above mentioned equation (for this the range of evaluation has to be limited to sufficient low temperatures, in general $T < 100$ K). This is motivated by the assumption that only acoustic phonons are thermally activated at lowest temperatures. In our case this evaluation would give $\theta_0 = 214$ K for $BaCeO_3$ and $\theta_0 = 235$ K for $BaZrO_3$, at $T = 0$ K. Based on the relationship between acoustic phonons of long wavelengths and elastic properties of the material [30], these Debye temperatures should be comparable to values (Θ_{elast}) calculated from elastic constants. Yamanaka et al. measured sound velocities of $BaCeO_3$ and $BaZrO_3$ at room temperature applying the pulse echo method [32]. From this they calculated the following (elastic) Debye temperatures: $\Theta_{elast} = 394$ K for $BaCeO_3$ and $\Theta_{elast} = 544$ K for $BaZrO_3$. There is large disagreement with our results. An uncertainty in the studies of Yamanaka et al. may originate from the fact that their ultrasound measurements were carried out on sintered pellets, estimating the data for 100% dense samples by means of finite element calculations. Surprisingly their data are closer to our results if N is set to 5. In this context it should be noted, that there are studies on other perovskites, which show as well a better coincidence between Θ_{elast} and θ_0, calculated without the restriction on acoustic phonons (i.e. not setting $N = 1$) [33–35]. At the moment we have no explanation for the better agreement in this case.

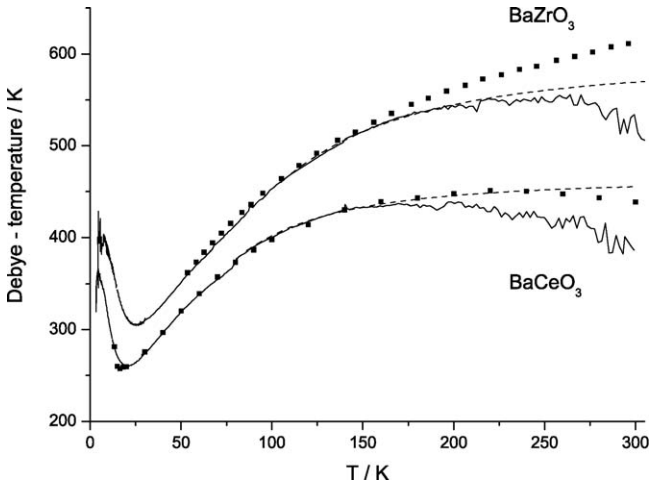

Fig. 3. Variation of the corresponding Debye temperatures Θ_D of $BaCeO_3$ and $BaZrO_3$ with temperature (C_p was normalised to the number of atoms per formula unit before conversion). Solid lines, present results; filled squares, data according to the measurement of Scholten and Schoonman ($BaCeO_3$) [8] and King and Weller ($BaZrO_3$) [9,10]; dashed lines, extrapolation of a harmonic fit (see text).

After attaining a maximum, the Debye temperatures of both substances start decreasing again, which in general is attributed to anharmonic lattice dynamics, not taken into account by the Debye theory. This behaviour is found for $BaZrO_3$ above 200 K, while it occurs at even lower temperatures (about 150 K) for $BaCeO_3$. To correct for anharmonicities we fitted a polynomial of the form $\theta_D^{-2}(T) = \theta_\infty^{-2}[1 + (a/T)^2 + (b/T)^4]$ to the temperature range, where harmonic behaviour is still assumed to be valid [36] (as the fit function is only of fourth order, the fit procedure was not extended below 80 K). The fitting results for θ_∞, denoting the high-T limit of the Debye temperature, are the following: $\theta_\infty = 464$ (±10) K for $BaCeO_3$ and $\theta_\infty = 592$ (±10) K for $BaZrO_3$. Extrapolation of the fit to elevated temperatures allows construction of the harmonic part of the heat capacity: by means of the Debye function, the Debye temperatures $\theta_D(T)$, calculated from the fit, can be converted into heat capacities. Values at selected temperatures are included in the diagram of Fig. 1 (filled squares). The excess heat capacity due to anharmonicity is directly related to the coefficient of thermal expansion [30] which is substantially larger for $BaCeO_3$ compared to $BaZrO_3$ as reported in literature [3,32,37,38]. This corresponds to the

more distinct deviation from harmonic behaviour in the case of $BaCeO_3$. It is basically the larger size of Ce^{4+}, compared to Zr^{4+}, that causes a less densely packed structure, respectively a less rigid lattice [39,40].

4. Conclusions

Our measurements of specific heat capacities provide corrected values for the heat capacity of $BaCeO_3$ in the range $T < 10$ K and fill the gap below 53 K in the case of $BaZrO_3$. Significant disagreement at elevated temperatures ($T > 150$ K) with data reported in literature has been detected as well. It is in general deplorable that for many important substances only a few studies on their low temperature properties exist.

Acknowledgements

The authors are grateful to A. Fuchs for assistance with the sample preparation and for SEM-EDX measurements, G. Goetz for performing the XRD analysis and E. Schmitt for technical support at the low temperature laboratory.

References

[1] F.T. Ewart, R.G. Taylor, J.M. Horspool, G. James, J. Nucl. Mater. 61 (1976) 254.
[2] H. Kleykamp, J.O. Paschoal, R. Pejsa, F. Thummler, J. Nucl. Mater. 130 (1985) 426.
[3] R. Vassen, X.Q. Cao, F. Tietz, D. Basu, D. Stover, J. Am. Ceram. Soc. 83 (2000) 2023.
[4] H. Iwahara, Solid State Ionics 77 (1995) 289.
[5] K.D. Kreuer, T. Dippel, Y.M. Baikov, J. Maier, Solid State Ionics 86–88 (1996) 613.
[6] D. Poulidi, M.A. Castello del Rio, R. Salar, A. Thursfield, I.S. Metcalfe, Solid State Ionics 162 (2003) 305.
[7] A. Erb, E. Walter, R. Flükiger, Physica C 245 (1995) 245.
[8] M.J. Scholten, J. Schoonman, J.C. van Miltenburg, E.H.P. Cordfunke, Thermochim. Acta 268 (1995) 161.
[9] E.G. King, W.W. Weller, Report BMI 5571 (1960).
[10] Y.S. Touloukian, E.H. Buyco, Thermophysical Properties of Matter, The TPRC Data Series, vol. 5, Specific Heat, Nonmetalic Solids, IFI, Plenum, New York, 1970.
[11] W. Schnelle, J. Engelhardt, E. Gmelin, Cryogenics 39 (1999) 271.
[12] E. Gmelin, Thermochim. Acta 110 (1987) 183.
[13] W. Schnelle, E. Gmelin, Thermochim. Acta 391 (2002) 41.
[14] K.S. Knight, Solid State Ionics 74 (1994) 109.
[15] H.C. Gupta, P. Simon, T. Pagnier, G. Lucazeau, J. Raman Spectrosc. 32 (2001) 3318.
[16] I. Levin, T.G. Amos, S.M. Bell, L. Farber, T.A. Vanderah, R.S. Roth, B.H. Toby, J. Solid State Chem. 175 (2003) 170.
[17] R.D. King-Smith, D. Vanderbilt, Phys. Rev. B 49 (1994) 5828.
[18] A.R. Akbarzadeh, I. Kornev, C. Malibert, L. Bellaiche, J.M. Kiat, Phys. Rev. B 72 (2005) 205104.
[19] M.E. Huntelaar, E.H.P. Cordfunke, R.R. van der Laan, Thermochim. Acta 274 (1996) 101.
[20] R. Saha, R. Babu, K. Nagarajan, C.K. Mathews, Thermochim. Acta 120 (1987) 29.
[21] T. Matsui, Thermochim. Acta 253 (1995) 155.
[22] R. Vankata Krishnan, N. Nagarajan, P.R. Vasudeva Rao, J. Nucl. Mater. 299 (2001) 28.
[23] I. Barin, Thermochimical Data of Pure Substances Pt. 1, VCH Verlagsgesellschaft mbH, Weinheim, 1993.
[24] O. Knacke, O. Kubaschewski, K. Hesselmann, Thermochimical Properties of Inorganic Substances, 2nd ed., Springer-Verlag, Berlin, 1991.
[25] S. Yamanaka, T. Hamaguchi, T. Oyama, T. Matsuda, S. Kobayashi, K. Kurosaki, J. Alloys Compd. 359 (2003) 1.
[26] P. Masri, L. Dobrzynski, Surf. Sci. 34 (1973) 119.
[27] E.S. Alber, J.L. Bassani, V. Vitek, G.J. Wang, Phys. Rev. B 53 (1996) 8398.
[28] A. Phillips, J. Low Temp. Phys. 7 (1972) 351.
[29] E. Gmelin, K. Guckelsberger, J. Phys. C: Solid State Phys. 14 (1981) L21.
[30] E.S.R. Gopal, Specific Heats at Low Temperatures, Plenum Press, New York, 1966.
[31] P. Roedhammer, W. Weber, E. Gmelin, K.H. Rieder, J. Chem. Phys. 64 (1976) 581.
[32] S. Yamanaka, M. Fujikane, T. Hamaguchi, H. Muta, T. Oyama, T. Matsuda, S. Kobayashi, K. Kurosaki, J. Alloys Compd. 359 (2003) 109.
[33] M. Hortal, S. Vieira, R. Villar, Ferroelectrics 54 (1984) 313.
[34] R. Villar, E. Gmelin, H. Grimm, Ferroelectrics 69 (1986) 165.
[35] S. Bourgeal, R. Villar, S. Vieira, V.A. Trepakov, Ferroelectrics 79 (1988) 237.
[36] T.H.K. Barron, W.T. Berg, J.A. Morrison, Proc. R. Soc. Lond. A 242 (1957) 478.
[37] K.C. Goretta, E.T. Park, R.E. Koritala, M.M. Cuber, E.A. Pascual, N. Chen, A.R. de Arellano-Lopez, J.L. Routbort, Phys. C 309 (1998) 245.
[38] A.V. Kuzmin, V.P. Gorelov, B.T. Melekh, M. Glerup, F.W. Poulsen, Solid State Ionics 162 (2003) 13.
[39] R. Terki, H. Feraoun, G. Bertrand, H. Aourag, phys. stat. solidi (b) 242 (2005) 1054.
[40] I. Charrier-Cougoulic, T. Pagnier, G. Lucazeau, J. Solid State Chem. 142 (1999) 220.